

Research Article

Metabolomic, lipidomic and proteomic characterisation of lipopolysaccharide-induced inflammation mouse model

Elena Puris, Štěpán Kouřil, Lukáš Najdekr, Seppo Auriola, Sanna Loppi, Paula Korhonen, Mireia Gómez-Budia, Gert Fricker, Katja M. Kanninen, Tarja Malm, David Friedecký, Mikko Gynther

PII: S0306-4522(22)00270-6
DOI: <https://doi.org/10.1016/j.neuroscience.2022.05.030>
Reference: NSC 20644

To appear in: *Neuroscience*

Received Date: 20 December 2021
Revised Date: 20 May 2022
Accepted Date: 23 May 2022

Please cite this article as: E. Puris, S. Kouřil, L. Najdekr, S. Auriola, S. Loppi, P. Korhonen, M. Gómez-Budia, G. Fricker, K.M. Kanninen, T. Malm, D. Friedecký, M. Gynther, Metabolomic, lipidomic and proteomic characterisation of lipopolysaccharide-induced inflammation mouse model, *Neuroscience* (2022), doi: <https://doi.org/10.1016/j.neuroscience.2022.05.030>

This is a PDF file of an article that has undergone enhancements after acceptance, such as the addition of a cover page and metadata, and formatting for readability, but it is not yet the definitive version of record. This version will undergo additional copyediting, typesetting and review before it is published in its final form, but we are providing this version to give early visibility of the article. Please note that, during the production process, errors may be discovered which could affect the content, and all legal disclaimers that apply to the journal pertain.



Metabolomic, lipidomic and proteomic characterisation of lipopolysaccharide-induced inflammation mouse model

Elena Puris^{a,b†}, Štěpán Kouřil^{c,d†}, Lukáš Najdekr^c, Seppo Auriola^a, Sanna Loppi^{e,f}, Paula Korhonen^e, Mireia Gómez-Budia^e, Gert Fricker^b, Katja M. Kanninen^e, Tarja Malm^e, , David Friedecký^{c,d}, Mikko Gynther^{a,b}*

^aSchool of Pharmacy, University of Eastern Finland, P.O. Box 1627, 70211 Kuopio, Finland

^bInstitute of Pharmacy and Molecular Biotechnology, Ruprecht-Karls-University, Im Neuenheimer Feld 329, 69120 Heidelberg, Germany (present address for E.P. and M.G.)

^cInstitute of Molecular and Translational Medicine, Palacký University Olomouc, Hněvotínská 5, 77900 Olomouc, Czech Republic

^dDepartment of Clinical Biochemistry, University Hospital Olomouc, I.P. Pavlova 6, 77900 Olomouc, Czech Republic

^eA.I. Virtanen Institute for Molecular Sciences, University of Eastern Finland, P.O. Box 1627, 70211 Kuopio, Finland

^fDepartment of Immunobiology, University of Arizona, 1656 E Mabel Street, Tucson, Arizona 85724-5221, USA (present address for S.L.)

†Elena Puris and Štěpán Kouřil should be considered joint first authors.

**corresponding author: Elena Puris, Institute of Pharmacy and Molecular Biotechnology, Ruprecht-Karls-University, Im Neuenheimer Feld 329, 69120 Heidelberg, Germany; phone: +(358)449789164; email: elena.puris@uni-heidelberg.de*

ABSTRACT

Neuroinflammation is an important feature in the pathogenesis and progression of central nervous system (CNS) diseases including Alzheimer's disease (AD). One of the widely used animal models of peripherally induced neuroinflammation and neurodegeneration is a lipopolysaccharide (LPS)-induced inflammation mouse model. An acute LPS administration has been widely used for investigation of inflammation-associated disease and testing inflammation-targeting drug candidates. In the present metabolomic, lipidomic and proteomic study, we investigated short-term effects of systemic inflammation induced by LPS administration on the mouse plasma and brain cortical and hippocampal metabolome, lipidome as well as expression of the brain cortical proteins which were shown to be involved in inflammation-associated CNS diseases. From a global perspective, the hippocampus was more vulnerable to the effects of LPS-induced systemic inflammation than the cortex. In addition, the study revealed several brain region-specific changes in metabolic pathways and lipids, such as statistically significant increase in several cortical and hippocampal phosphatidylcholines/ phosphatidylethanolamines, and significantly decreased levels of brain cortical betaine after LPS treatment in mice. Moreover, LPS treatment in mice caused significantly increased protein expression of GluN1 receptor in the brain cortex. The revealed perturbations in the LPS-induced inflammation mouse model may give insight into the mechanisms underlying inflammation-associated CNS diseases. In addition, the finding of the study provide important information about the appropriate use of the model during target validation and drug candidate testing.

Keywords: Alzheimer's disease, lipopolysaccharide; metabolomics; lipidomics; proteomics

Introduction

Neuroinflammation, defined as an inflammatory response within the brain or spinal cord, is a critical feature in the pathogenesis and progression of central nervous system (CNS) diseases including neurodegenerative disorders such as Alzheimer's disease (AD) (Kwon and Koh, 2020). Neuroinflammation is mediated by the production of cytokines, chemokines, reactive oxygen species, and secondary messengers, which are produced by microglia and astrocytes, endothelial cells, and peripherally derived immune cells (DiSabato et al., 2016). Understanding of the inflammatory mechanisms has driven breakthroughs in therapy of several CNS diseases, resulting in development of effective immunosuppressive drugs (Gilhus and Deuschl, 2019). In addition, it has been recently reported that inflammation resulted from peripheral infections play important role in the development of sporadic AD. Therefore, targeting peripheral inflammation was considered as a promising treatment approach for this neurodegenerative disease (Giridharan et al., 2019).

For the purpose of the development of new therapeutic treatments and testing of potential drug candidates targeting inflammation, inflammation-induced animal models can be very useful. One of the widely used animal models of peripherally induced neuroinflammation and neurodegeneration is a lipopolysaccharide (LPS)-induced inflammation mouse model (Catorce and Gevorkian, 2016). LPS is a cell wall immunostimulatory component of the outer membrane of Gram-negative bacteria and a potent endotoxin stimulating a persistent inflammation (Alexander and Rietschel, 2001). Systemic administration of LPS, a Toll-like receptor 4 (TLR-4) ligand, even at low doses, causes a robust induction of various pro-inflammatory cytokines in macrophages through the TLR-4 pathway (Maitra et al., 2012, Beutler, 2000). TLR-4 is primarily expressed in microglia, which are the resident macrophages in the brain. TLR-4 activation by LPS induces the production of pro-inflammatory cytokines, such as TNF- α , IL-1 β , and prostaglandin E₂ (PGE₂), mediating the neuroinflammatory process (Lehnardt et al., 2002, Mrak and Griffin, 2005). Peripheral administration of LPS lead to cognitive impairment in mice (Zhao et al., 2019). In addition, it has been previously demonstrated that repeated intraperitoneal administration of LPS (250 μ g/kg) for 3 to 7 days resulted in accumulation of A β ₁₋₄₂ in the mouse hippocampus and cerebral cortex through increased β - and γ -secretase activities accompanied with the increased expression of amyloid precursor protein (APP) (Lee et al., 2008). These findings support the evidence of involvement of inflammatory response in AD development. Therefore, an acute peripheral LPS administration has been frequently used to study neuroinflammation-associated diseases in mice such as AD as well as

neuroinflammation targeting drug candidates (Ghosh et al., 2020, Li et al., 2021, Manouchehrian et al., 2021, Li et al., 2020).

Metabolites and lipids are important building blocks for cellular components, as well as signalling molecules maintaining the normal functioning of the biological systems. Several studies have been conducted to investigate either metabolic or lipidomic changes due to LPS-induced inflammation in mice with the main focus on single biological matrix (Wu et al., 2016, Piirsalu et al., 2020, Cani et al., 2007). The systematic knowledge of short-term effects due to peripheral LPS administration on mouse brain lipidome and metabolome would allow the more rational use of the model in neuroinflammation drug research.

In the present study, we investigated the short-term effects of LPS-induced systemic inflammation on the mouse plasma and brain cortical and hippocampal metabolome, lipidome and expression of the brain cortical proteins which were shown to be involved in inflammation and/or inflammation-associated neurodegenerative diseases such as AD (Puris et al., 2021a). For this purpose, mice were intraperitoneally injected with LPS according to previously published protocol, which demonstrated effectiveness in generating systemic inflammation, induction of memory impairment and accumulation of A β ₁₋₄₂ in the hippocampus and cerebral cortex of wild-type mice (Lee et al., 2008). We compared the plasmatic, brain hippocampal and cortical metabolome and lipidome in LPS-treated wild-type mice to age-matched saline-treated wild-type mice using two comprehensive analytical approaches such as targeted metabolomics and untargeted lipidomics. These approaches enabled to cover major metabolic pathways and to obtain a general overview of altered lipid classes and species. Additionally, we investigated the changes in protein expression of ATP-binding cassette transporters (ABC) and solute carrier (SLC) transporters, ionotropic glutamate receptor subunit 1 (GluN1), enzymes monoacylglycerol lipase (Mgl1) and cyclooxygenase 2 (Cox-2) in crude membrane fractions of the brain cortical tissue of LPS-treated mice compared to age-matched saline-treated mice. To achieve this goal, we used previously developed liquid chromatography tandem mass spectrometry (LC-MS/MS) based quantitative targeted absolute proteomic (QTAP) method (Puris et al., 2021a).

Experimental procedures

Study design and animals

The animal experiments complied with the ARRIVE guidelines and were conducted according to EU Directive 2010/63/EU for animal experiments. The procedures including the animal use were approved by the Finnish National Animal Experimental Board (ESAVI-2015-000744). The animals were housed under standard laboratory conditions: 12-12 h light-dark day cycle;

four to six animals per cage; food (Lactamin R36; Lactamin AB, Södertälje, Sweden) and water consumption *ad libitum*, 60% relative humidity. The study inclusion and exclusion criteria were based on the animal health state; only healthy animals which showed no signs of illness as evaluated by the body weight and visual observations were used.

In the study, adult female C57BL/6J mice (fifteen-week-old) were used. The animals were administered either 250 µg/kg LPS (#L2880, Sigma-Aldrich) (referred to as wild-type WT plus LPS group) or sterile saline (0.9% NaCl) solution (WT control group) i.p. once per day for three days followed by decapitation on fourth day. The LPS treatment regimen was selected based on previous report showing that daily LPS (250 µg/kg) i.p. injections for 3 days resulted in the brain hippocampal and cortical accumulation of A β ₁₋₄₂ through increased β - and γ -secretase activities accompanied with the increased expression of APP as well as activation of astrocytes in mice (Lee et al., 2008). On the decapitation day (24 h after the last LPS injection), the mice were anaesthetised by tribromoethanol (#75-80-9, Avertin, Sigma-Aldrich, St. Louis, MO, USA), a terminal anaesthetic providing fast and deep surgical analgesia, which use was approved by the Finnish National Animal Experimental Board (ESAVI-2015-000744). After anaesthesia, the blood was collected by cardiac puncture into tubes containing citrate as an anticoagulant, and the plasma was obtained by centrifugation at 1500 × g for 6 min followed by centrifugation of the plasma layer at 12000 × g to remove the platelets. The plasma was stored at -80 °C until the analysis. The mouse brains were perfused transcardially with heparinised saline (2500 IU/L) for 3 min. The meninges were removed, and the brain cortex and hippocampus were separated, snap-frozen in liquid nitrogen, and stored at -80 °C until the analysis. In addition, the spleen samples were collected and snap-frozen in liquid nitrogen, and stored at -80 °C until the cytokine analysis.

With respect to the required power of the study set to 0.8 and alpha to 0.05, the effect size of 1.1 and higher was calculated (Statistica 14.0.0.15, TIBCO software) as statistically significant for sample size (n = 9 per group) in the metabolomic and lipidomic study. The sample size was set as a compromise between the complexity of the experiment, the use of animal models in the study and the general recommendation for metabolomic studies. The sample size (n = 5) selection for the proteomics analysis was based on previously reported QTAP studies in mice (n = 3). (Pan et al., 2018, Pan et al., 2019, Puris et al., 2021a)

Metabolomic and lipidomic experiment

Plasma sample preparation

For targeted metabolomics, plasma samples were prepared based on a previously described protocol (Yuan et al., 2012). Briefly, plasma samples (30 µL) were centrifuged (14000 × g; 10

min; 4 °C) and supernatants (20 µL) were mixed with pre-chilled methanol (80 µL). The samples were stored for 6 h at -80 °C. After the centrifugation (14000 × g; 10 min; 4 °C), the supernatant (80 µL) was freeze-dried. Finally, the samples were resuspended in methanol/water (4:1; vol/vol; 100 µL), vortexed (30 s), centrifuged (at 20000 × g for 10 min at 4 °C) and transferred into HPLC glass vials with inserts.

Samples for lipidomics were prepared using a extraction protocol adapted from Sarafian et al. (2014) (Sarafian et al., 2014). The plasma samples (25 µL) were mixed with a mixture of methanol/tert-butyl methyl ether/water (187.5 µL; 1:5:1.5; vol/vol/vol), vortexed (60 s), and left at laboratory temperature (10 min). After overnight incubation (-20 °C), the samples were centrifuged (14000 × g; 20 min; 4 °C), and the organic phase (120 µL) was freeze-dried. The final reconstitution was done by the same procedure as the samples for the metabolomic analysis using propan-2-ol/acetonitrile/water (2:1:1; vol/vol/vol, 120 µL).

Tissue sample preparation

The mouse cortex and hippocampus samples were prepared according to the previously published method (Vorkas et al., 2015). For metabolomic analysis, frozen cortex and hippocampus samples (26.2 ± 4.26 mg) were mixed with pre-chilled methanol/water (-80°C; 1:1; 100 µL of solvent per 28 mg of tissue) and homogenized (TissueLyser II, QIAGEN; 5-mm steel bead; 30 times/s; 40 s; 2 plus 2 cycles). The samples were centrifuged (13000 × g; 20 min; 4 °C) and supernatant (100µL) was freeze-dried. The samples were consequently processed in the same manner as plasma samples. For lipidomic analysis, pre-chilled dichloromethane/methanol (-80 °C; 3:1; 100 µL of solvent per 28 mg of tissue) was mixed with the residual pellet left from aqueous extraction. The samples were again homogenized and centrifuged under the same conditions. The supernatant (28 mg of tissue/100 µL of aliquot) were transferred into glass vials, left in an extractor hood overnight for evaporation at laboratory temperature. The samples were consequently processed in the same way as plasma samples.

Quality control samples

A pooled quality control (QC) sample was prepared by combining aliquots (10 µL) from each sample. Extract blanks were prepared in the same way as regular samples, using water instead of plasma or tissue.

Targeted metabolomics and untargeted lipidomics

The LC/MS method for targeted metabolomic experiments was adopted from Yuan et al. (2012) (Yuan et al., 2012). The list of measured analytes and their MRM transitions is provided in Supplementary Table S1. The samples were separated on a Phenomenex Luna NH₂ column (2.1 × 150 mm, 3 µm, Phenomenex, UK) using mobile phase A (20 mM ammonium acetate in water;

pH 9.75) and mobile phase B (acetonitrile). The flow rate was set to 0.30 mL/min with the following gradient: $t=0.0$, 95% B; $t=15.0$, 30% B; $t=17.0$, 5% B; $t=23.0$, 5% B; $t=23.1$, 95% B; $t=28.0$ min 95% B. The column temperature was set to 35 °C, and the injection volume was 2 μ L. The MS parameters were as follows: the ion spray voltage was +5500 V and -4500 V; curtain gas 40 psi; both ion source gases were 40 psi; ion source temperature 400 °C. To control the LC/MS instrument the Analyst 1.6.2 software (SCIEX) was used.

The untargeted lipidomic experiments were done on liquid chromatograph-mass spectrometer using a Dionex UltiMate 3000 RS (Thermo Fisher Scientific, MA, USA) coupled with an Orbitrap Elite (Thermo Fisher Scientific, MA, USA). Samples were separated on an Acquity UPLC BEH C18 column, (2.1 \times 100 mm, 1.7 μ m; Waters Corp, USA) using a modified previously published method (Vorkas *et al.* 2015). The gradient elution consisting of mobile phase A (10 mM ammonium formate and 0.1% formic acid in 60% acetonitrile/water) and mobile phase B (10 mM ammonium formate and 0.1% formic acid in 90% propan-2-ol/water) was applied. The flow rate was set to 0.40 mL/min with the following gradient: $t=0.0$, 40% B; $t=2$, 43% B, $t=2.1$, 50% B; $t=12.0$, 54% B; $t=12.1$, 70% B; $t=18.0$, 99% B; $t=18.1$, 40% B; $t=20.0$, 40% B. The column temperature was set to 55 °C, and the injection volume was 2 μ L. The data was acquired in positive ionisation mode (mass range of 100-1600 m/z) at a resolution of 60000 FWHM. The ion source parameters were set as follows: the sheath gas was 40 arbitrary units; the aux gas was 15 arbitrary units; the spray voltage was 3 kV; the capillary temperature was 300 °C; the source heater temperature was 350 °C. A Thermo Tune Plus 2.7.0.1103 SP1 was used as the instrument control software for the Orbitrap Elite, and the data was acquired in centroid mode.

For the purpose of conditioning and stability correction of the mass spectrometry instruments the QC samples were analysed as the first ten injections and then every sixth injection with two QC samples at the end of the analytical batch. Two blank samples were analysed, the first as the sixth injection and then at the end of each batch.

Quantitative targeted absolute proteomic analysis

The absolute protein expression levels of membrane transporters P-glycoprotein (P-gp, encoded by *Abcb1a/b*), multidrug resistance-associated protein 1 (Mrp1, encoded by *Abcc1*), Mrp4 (encoded by *Abcc4*), breast cancer resistance protein (Bcrp, *Abcg2*), glucose transporter 1 (Glut1, *Slc2a1*), L-type amino acid transporter 1 (Lat1, *Slc7a5*), as well as membrane bound enzymes cyclooxygenase 2 (Cox-2), monoacylglycerol lipase (Mgl1), ionotropic glutamate receptor subunit 1 (GluN1) and membrane marker Na⁺/K⁺-ATPase were measured in the isolated crude membrane fractions of the mouse brain cortices as described previously (Puris et

al., 2021a). Briefly, the crude membranes were isolated using ProteoExtract Subcellular Proteome Extraction Kit (Merck KGaA, Darmstadt, Germany) according to the manufacturer's protocol. The total protein concentrations in the extracted crude membrane fractions were measured using the BioRad Protein Assay. The sample aliquots of 50 μg protein were used for sample preparation, which was performed according to the previously published protocol (Uchida et al., 2013). The proteins in the samples were solubilized in 7 M guanidine hydrochloride, 500 mM Tris-HCl (pH 8.5) and 10 mM EDTA and reduced with dithiothreitol followed by *S*-carbamoylmethylation with iodoacetamide. The proteins were precipitated with methanol and chloroform and dissolved by addition of 6 M urea in 0.1 M Tris-HCl (pH 8.5) followed by a dilution with 0.1 M Tris-HCl (pH 8.5) containing a mixture of stable isotope-labelled peptide purchased from JPT Peptide Technologies GmbH (Berlin, Germany) (Supplementary Table S2). After addition of Lys-C and Protease-Max (Promega, Madison, WI, USA), the samples were incubated at room temperature for 3 h. Finally, tosylphenylalanyl chloromethyl ketone-treated trypsin was added to the samples (enzyme/substrate ratio of 1:100) for tryptic digestion, which occurred during the incubation at 37 °C for 16 h. Formic acid in water 20% (v/v) was used to acidify the samples, followed by centrifugation at 14000 $\times g$ for 5 min at 4 °C. The supernatants were analyzed using previously published LC-MS/MS methods (Puris et al., 2021a, Uchida et al., 2011, Uchida et al., 2013). The quantification of a stable isotope-labelled peptide and the unlabelled investigated peptide was based on three or four MRM transitions for each specific peptide related to high intensity fragment ions (Supplementary Table S2). The mean of the ratios of light to heavy peaks for each MRM transition were used for quantification with a dot-product value between the peak areas equal to 1. The expression of target proteins in crude membrane fractions of mouse brain cortical tissues were expressed as absolute values (fmol/ μg total protein in crude membrane).

Cytokine analysis

The cytokine analysis of the mouse spleen, plasma and brain cortical samples was performed to elucidate whether the changes in the brain metabolome, lipidome as well as protein expression are resulted by systemic inflammation and/or neuroinflammation. Tissue homogenising buffer consisting of diethyl pyrocarbonate (DEPC) water, 20 mM Tris-HCl (pH 7.5), 250 mM sucrose, 5 mM EDTA, 10 mM EGTA, and a protease inhibitor cocktail (1:200) was added to the spleen samples in the proportion of 8 μL per mg spleen or brain cortical tissue. The tissue was homogenised with a bead beater (TissueLyser II, QIAGEN) at 30 Hz for 2 min at 4 °C. The homogenised tissue was centrifuged at 14000 $\times g$ at 4 °C for 10 min. The supernatant was transferred to a new tube and stored at -80 °C until the analysis. The protein

concentrations in the samples were measured using a Pierce BCA Protein Assay Kit, and the results of the Cytometric Bead Array (CBA) were normalised to the total protein concentrations of the samples. The cytokine analysis of the mouse spleen, brain cortical tissue and plasma samples was performed with a BD Cytometric Bead Array mouse inflammation kit (BD Biosciences San Diego, CA, USA) according to the manufacturer's protocol. The levels of interleukins (IL-6, IL-10, IL-12p70), interferon- γ (IFN- γ), monocyte chemoattractant protein-1 (MCP-1) and tumour necrosis factor α (TNF- α) in the plasma and spleen samples were measured. The samples were run with CytoFLEX S, and the results were analysed with the FCAP Array 2.0.0 software (Soft Flow Hungary Ltd, Pecs, Hungary).

Quantitative Real-Time Polymerase Chain Reaction analysis

Quantification of gene expression in mouse brain cortical and hippocampal tissues was performed using quantitative real-time polymerase chain reaction (qRT-PCR). The following genes were studied: glial fibrillary acidic protein (Gfap), allograft inflammatory factor 1 (Aif1, also known as ionized calcium-binding adapter molecule 1, Iba1), β -secretase 1 (Bace1), Presenilin-1 (Psen1), γ -secretase subunit APH-1A (Aph1a) and γ -secretase subunit APH-1B (Aph1b). Total RNA was extracted from mouse brain cortical and hippocampal tissues using the RNeasy Mini Kit (Qiagen, Stockach, Germany) in accordance with the manufacturer's instructions followed by quantification by a NanoDrop (Thermo Scientific, Dreieich, Germany). Subsequently, cDNA was synthesized using Biozym cDNA Synthesis Kit (Biozym Scientific GmbH, Germany) according to the manufacturer's protocol. The synthesized cDNA was mixed with the PowerUp SYBR Green MasterMix (Life Technologies) and various sets of gene-specific validated primers (Supplementary Table S3) purchased from (ThermoFisher Scientific). Normalized relative expression per sample was calculated by dividing the relative quantity of a given target/sample by the geometric mean of the relative quantities of housekeeping gene β -actin according to Taylor et al. (2019) (Taylor et al., 2019). The qRT-PCR was performed using a LightCycler 96 (Roche Diagnostics), and the data were acquired using LightCycler® 96 SW 1.1 software, v. 1.1.0.1320 (Roche Diagnostics, Mannheim, Germany; 2011).

Data analysis and statistics

Integration of the peaks of the targeted metabolomics data was performed using MultiQuant 3.0 (SCIEX). Raw data sets from the untargeted lipidomic analysis were preprocessed using the vendor's Compound Discoverer 3.0 software (Thermo Fisher Scientific), including RT alignment, peak selection, adduct annotation, and blank subtraction. Removal of fragments from the source was performed using the R script CROP (Kouril et al., 2020). Data processing

and statistical evaluation was performed using the R package Metabol (Team, 2013). Quality control-based LOESS regression was used (Dunn et al., 2011). Based on coefficients of variation (CVs) calculated from QC samples, metabolites/features with CVs greater than 30% were excluded from further data processing. The data were analyzed as compositions using log-centered coefficients (clr) and centering of means (Pawlowsky-Glahn and Buccianti, 2011). Both multivariate unsupervised principal component analysis (PCA) and supervised discriminant analysis (PLS-DA) as well as univariate statistical methods (heatmaps based on p -values, box plots) were used. The p -value was calculated using a t -test and a Bonferroni correction was applied. The presence of outliers was evaluated by outlier detection in the interquartile range and visual inspection of the results from multivariate statistics. The most altered biochemical pathways and their comparisons for all groups examined were determined using the MetaboAnalyst 4.0 Pathway Analysis module. In order to identify and compare the most significant pathways, the $-\log(p\text{-value})$ threshold was set to 3.0 and the pathway impact value threshold was set to 0.3 (highlighted by the red rectangle in the graphs). The Global Test and Relative-betweenness Centrality algorithms were used. Features from untargeted lipidomic analyses were annotated by online Lipid Maps search (mass tolerance < 10 ppm) and manually by the Metlin database (statistically significant features, mass tolerance < 1 ppm, corresponding retention time behavior). Some of the statistically discriminating lipids, i.e., lysophosphatidylcholines (LPC)/ lysophosphatidylethanolamines (LPE) and phosphatidylcholines (PC)/ phosphatidylethanolamines (PE), were not distinguished because of the same molecular weight and retention time behavior.

The absolute protein expression levels are presented as mean \pm standard deviation (SD). Statistical significance between WT control group and WT plus LPS group was analysed by unpaired t -test. A p -value less than 0.05 was considered statistically significant. Data analysis was done using GraphPad Prism, version 5.03 (GraphPad Software, San Diego, CA).

For the statistical analysis of the differences in cytokine levels (IL-6, IL-10, MCP-1, IFN- γ , TNF- α , and IL-12p70) of the spleen, brain cortex and plasma between the groups, i.e. the WT plus LPS versus WT controls, unpaired t -test was used (GraphPad Prism, version 5.03, GraphPad Software, San Diego, CA). Statistical significance was defined as $p < 0.05$.

Results

Cytokine analysis

The cytokine analysis demonstrated significantly increased production of MCP-1 ($p = 0.001$) and IL-12p70 ($p = 0.03$) in the spleen of WT plus LPS group compared to WT controls (Fig. 1A). In the plasma, the levels of MCP-1 and TNF- α were significantly higher ($p = 0.02$ for both

cytokines) in the WT plus LPS group compared to WT controls (Fig. 1B). There were no other significant changes observed in the levels of investigated cytokine in plasma and spleen of the WT plus LPS group compared to WT controls (Fig. 1A, B). In the brain cortical tissue of LPS-treated mice, only the levels of MCP-1 (0.63 ± 0.16 pg/ μ g protein) and IL-12p70 (0.040 ± 0.18 pg/ μ g protein) were detected, while in WT control group, the levels of these and other cytokines were below the quantification limit (IL-6 < 6.3 pg/mL, IL-10 < 2.4 pg/mL, MCP-1 < 19.0 pg/mL, IFN- γ < 5.8 pg/mL, TNF- α < 5.8 pg/mL, and IL-12p70 < 7.7 pg/mL).

Gene expression in mouse brain hippocampal and cortical tissues

The changes in normalized mRNA expression of inflammation markers as well as β -secretase and γ -secretase in the cortical and hippocampal tissues of WT plus LPS group and WT controls were investigated using qRT-PCR (Fig. 2). The normalized mRNA expression of astrocytic and microglial activation markers, i.e., Gfap and Aif1, was significantly increased in the hippocampal tissue of WT plus LPS group compared to WT controls ($p < 0.05$) (Fig 2A). In addition, LPS treatment resulted in significantly increased normalized mRNA expression of Bace1 ($p = 0.008$), Psen1 ($p = 0.01$), Aph1a ($p = 0.006$), but not Aph1b in the hippocampal tissue of WT mice compared to WT control group. In contrast, the normalized mRNA expression of the investigated genes (Gfap, Aif1, Bace1, Psen1, Aph1a/b) was not significantly altered in the cortical tissue of WT plus LPS group compared to WT controls (Fig. 2B).

Targeted metabolomic and untargeted lipidomic analyses

The targeted metabolomic analysis in the brain cortex and hippocampus of WT plus LPS group and WT controls resulted in the detection of 153 metabolites (Supplementary Table S4). The untargeted lipidomic analysis in the brain cortex and hippocampus of WT plus LPS group and WT controls resulted in the detection of 1435 features (Supplementary Table S5). In mouse plasma of both study groups, 147 metabolites and 952 lipids were detected (Supplementary Tables S6, S7).

The unsupervised multivariate statistical method, such as principal component analysis (PCA) was used for study of overall differences and similarities in the hippocampal and cortical metabolites and lipids between the WT plus LPS group and WT controls (Fig. 3, Supplementary data file 1). The study groups displayed better separation in the metabolome and lipidome of the hippocampus (Fig. 3 B, E) than the cortex (Fig. 3A, D) suggesting that the hippocampus is more affected by LPS treatment than the cortex. The comparison of the plasmatic profiles of WT control and WT plus LPS group revealed separation metabolome and lipidome between the groups (Fig. 3C, F).

The biochemical pathway analysis (Fig. 4) demonstrated similar findings to those observed in the unsupervised PCAs described above, such as more affected metabolome of the WT plus LPS group vs. WT controls in the hippocampus compared to the cortex. The administration of LPS in mice resulted in alterations of several metabolic pathways in both the cortex and hippocampus (Fig. 4), as follows: glycine, serine, and threonine metabolism; cysteine and methionine metabolism; riboflavin metabolism; arginine and proline metabolism; pyrimidine metabolism; nicotinate and nicotinamide metabolism. In addition, the following pathways were altered in the hippocampus of the WT plus LPS group as compared to the WT control group: alanine, aspartate, and glutamate metabolism; carbohydrate metabolism; arginine biosynthesis; purine metabolism; glutathione metabolism. The changes in taurine and hypotaurine metabolism were observed only in the cortex of the WT plus LPS group as compared to the WT control group. Similarly to the brain, the most affected metabolic pathways in the plasma were as follows: glycine, serine, and threonine metabolism; cysteine and methionine metabolism; arginine and proline metabolism. However, the changes in phenylalanine metabolism and citrate cycle (TCA cycle) were plasma-specific, and were not observed in the brain cortex and hippocampus of the WT plus LPS group as compared to the WT control group.

We constructed a *p*-value based heatmap to shed light on the individual metabolic pathways that were altered in the brain cortex, hippocampus and plasma due to LPS administration in mice (Fig. 5, Supplementary Fig. S1). A gradual increase of statistical significance is demonstrated as a decrease in the *p*-value (Fig. 5, Supplementary Fig. S1) for metabolites in the WT plus LPS mice compared to the WT mice. The analysis demonstrated various changes in the brain cortex, hippocampus and plasma in the WT plus LPS compared to the WT controls. The LPS administration resulted in significant decrease in betaine levels in the cortex of the mice. The significant increase in cysteine and cystine was observed in the plasma of the WT plus LPS compared to the WT controls (Fig. 5, Supplementary Tables S4 and S6). Most acylcarnitines showed increasing trend in the cortex of the WT plus LPS group compared to the WT controls, while in the hippocampus and plasma several acylcarnitines demonstrated decreasing trend due to LPS treatment in mice (Fig. 5).

A *p*-value based heatmap of the most affected lipids in the brain cortical and hippocampal tissue was constructed (Fig. 6). The following affected lipid classes were selected to display the general changes due to LPS treatment in mice (Fig. 6): phosphatidylcholines/phosphatidylethanolamines (PCs/PEs), lysophosphatidylcholines/lysophosphatidylethanolamines (LPCs/LPEs), diacylglycerols (DGs), triacylglycerols (TGs). The levels of diacylglycerols (DGs) showed increasing trend specifically in the hippocampus

of the WT plus LPS group compared to the WT control group, while TGs showed an increasing trend only in the brain cortex of the WT plus LPS group as compared to the WT controls. The statistically significant increase was observed only in TG50:2 levels in the brain cortex of the WT plus LPS group compared to the WT controls. Various changes in PCs/PEs were found in the cortex and hippocampus of the WT plus LPS group compared to the WT controls. Thus, LPS administration lead to statistically significant increase in the cortical levels of PC aa C33:3/PE aa C36:3, PC ae C34:3/PE ae C37:3, PC aa C34:2/PE aa C37:2 as well as the cortical and hippocampal levels of PC ae C34:2/PE ae C37:2 in mice (Fig. 6, Supplementary Table S7). There were no statistically significant changes in the LPCs/LPEs in the cortex and hippocampus of the WT plus LPS group compared to the WT controls. The untargeted lipidomic analysis of plasma revealed significantly increased levels of PC(P-36:2)/PC(O-36:3), PC(P-34:1)/PC(O-34:1)/PE(P-37:1)/PE(O-37:2), PC(P-34:0)/PC(O-34:1)/PE(P-37:0)/PE(O-37:1) and glucosylceramide GlcCer(34:1) as well as significantly decreased levels of PC(O-42:6) in the WT plus LPS group compared to the WT controls (Supplementary Table S7). No other statistically significant changes in plasmatic lipids were observed in the study groups.

Targeted proteomic analysis

The absolute protein expression of the drug transporters (P-gp, Mrp1, Mrp4, Bcrp, Glut1, Lat1), membrane bound enzymes (Cox-2, Mgll), receptor GluN1 measured in crude membrane fractions of the brain cortical tissues of the WT plus LPS group compared to the WT controls and presented in Table 1. The absolute protein expression of membrane marker protein Na⁺/K⁺-ATPase did not differ between the WT plus LPS group (143.4 ± 30.9 fmol/μg protein) and the WT controls (155.0 ± 29.4 fmol/μg protein) providing the evidence of comparable crude membrane fraction enrichment.

The mean protein expression of GluN1 was significantly increased in the WT plus LPS group ($p = 0.003$) compared to the WT control mice (Table 1). There were no statistically significant differences in the protein expression of Mgll and Cox-2 in the crude membrane fraction of the brain cortical tissues between the all study groups (Table 1). There were no statistically significant differences in the mean protein expression of drug transporters P-gp, Bcrp, Mrp1, Mrp4, Glut1 and Lat1 between the WT plus LPS group and the WT controls (Table 1).

Table 1. Comparison of absolute protein expression levels (fmol/ μ g protein) of the investigated proteins in the isolated crude membrane fraction of the brain cortical tissue of wild-type (WT) mice treated with LPS (n = 5) versus WT control group (n = 5).

Protein name	WT control	WT plus LPS	Ratio to control	<i>p</i> value
	Mean \pm SD fmol/ μ g protein	Mean \pm SD fmol/ μ g protein		
GluN1	0.050 \pm 0.0080	0.070 \pm 0.002	1.4	< 0.01
Mgl1	6.4 \pm 2.1	5.7 \pm 1.4	0.89	0.58
Cox-2	0.11 \pm 0.040	0.080 \pm 0.040	0.72	0.36
P-gp	0.59 \pm 0.18	0.58 \pm 0.24	0.98	0.93
Bcrp	0.39 \pm 0.15	0.38 \pm 0.070	0.97	0.94
Mrp1	0.23 \pm 0.050	0.27 \pm 0.060	1.2	0.32
Mrp4	0.020 \pm 0.0050	0.020 \pm 0.001	1.0	0.35
Glut1	3.7 \pm 1.6	3.2 \pm 0.74	0.84	0.47
Lat1	0.24 \pm 0.020	0.23 \pm 0.10	0.95	0.93

Discussion

Recent clinical and preclinical studies suggest that systemic inflammation, which is resulted from peripheral infections and leads to production of cytokines circulating in the blood and communicating with the CNS, may contribute to the outcome or progression of chronic neurodegenerative diseases, in particular AD (Sly et al., 2001, Puris et al., 2021b, Holmes et al., 2003, Puris et al., 2021a). In the present study, we investigated the short-term effects of systemic inflammation induced by LPS administration on the mouse brain and plasma metabolome and lipidome as well as protein expression of several inflammation- and AD-related proteins in the mouse brain cortical tissue. The treatment with LPS in mice resulted in elevated production of proinflammatory cytokines in the spleen and in plasma providing the evidence of systemic inflammation. Moreover, we observed increased levels of β - and γ -secretases and activated microglia and astrocytes in the mouse hippocampus, but not cortex indicating LPS-induced A β pathology and inflammation in this brain region. In the present comprehensive -omics study, we characterise the changes in the plasma and brain cortical and hippocampal metabolome, lipidome and expression of several proteins triggered by systemic inflammation induced by LPS administration in mice.

Region-specific changes in metabolome and lipidome

From a global perspective, after comparing the metabolic and lipidomic profile in LPS- and saline-treated mice, the study revealed that the hippocampus is more vulnerable to be affected by LPS-induced systemic inflammation than the cortex. The greater number of affected metabolic pathways were observed in hippocampal metabolome than in the brain cortical or

plasmatic metabolomes in mice after LPS treatment. These region-specific alterations can be associated to LPS-induced activation of microglial cells and astrocytes as well as increased expression of β - and γ -secretases in the mouse brain hippocampus, which have been shown to result in increased activities of these enzymes leading to accumulation of A β (Li et al., 2011, Coulson et al., 2010). The hippocampus is responsible for learning and memory functions, and serves as a major site of adult neurogenesis (Zhao et al., 2008). In addition, the hippocampus, is especially vulnerable to damage in neurodegenerative disorders such as AD (Mu and Gage, 2011). Interestingly, in our previous study, chronic LPS treatment had greater impact on hippocampal metabolome of the APdE9 mice compared to cortex (Puris et al., 2021b). In another study, peripheral inflammation affected hippocampal neurogenesis in mice (Zonis et al., 2015). Together, these results indicate that the hippocampus is more susceptible to alterations triggered by the systemic inflammation compared to the cortex.

Although several biochemical pathways (glycine, serine, and threonine metabolism; cysteine and methionine metabolism; arginine and proline metabolism; pyrimidine metabolism; nicotinate and nicotinamide metabolism; riboflavin metabolism) were altered in both mouse cortex and hippocampus after LPS administration, some of the changes were region-specific. For instance, alanine, aspartate, and glutamate metabolism; carbohydrate metabolism; arginine biosynthesis; purine metabolism; glutathione metabolism were altered in hippocampus, while taurine and hypotaurine metabolism were affected only in the cortex. Similar to our findings, the changes in arginine and proline metabolism were found in the prefrontal cortex of mice after i.p. injection LPS injection at a dose of 0.83 mg/kg (Wu et al., 2016). In the same study the changes in alanine, aspartate, and glutamate metabolism were observed in the prefrontal cortex of LPS-treated mice (Wu et al., 2016), while in our study these changes were hippocampus-specific. The metabolic alterations observed in the brains of the LPS treated mice were not reflected in the plasma.

A closer look at the metabolic profile in mice after LPS administration revealed significant changes in the levels of several metabolites. For instance, levels of methyl-donor betaine regulating phospholipid metabolism were significantly decreased in the cortex of the mice after LPS treatment compared to saline-treated controls. Betaine possesses anti-inflammatory effects via amelioration of sulfur amino acid metabolism against oxidative stress, nuclear factor- κ B activity inhibition and regulation of energy metabolism (Zhao et al., 2018). The deficiency of betaine can lead to the impairment of methylation metabolism in the elderly, which is a risk factor for AD (Selhub et al., 2000, Obeid, 2013). LPS-induced systemic inflammation in mice lead to increased plasmatic levels of cysteine and its disulfide, cystine, which are the major

extracellular thiol/disulfide redox control system. The oxidation of steady-state redox potential (E_h) of cysteine/cystine is implicated in acute and chronic inflammatory disease states. Iyer et al (2009) demonstrated that E_h cysteine/cystine in human plasma are associated with IL-1 β levels (Iyer et al., 2009).

Most acylcarnitines showed statistically insignificant increasing trend in the cortex of the mice treated with LPS compared to saline-treated animals, while in the hippocampus and plasma the majority of acylcarnitines demonstrated decreasing trends after LPS treatment in mice. In the brain, acylcarnitines have a multifunctional role, including lipid synthesis, improving mitochondrial function, increasing antioxidant activity, and neuroprotection (Jones et al., 2010). The present study demonstrated some discrepancies between the changes in cortical, hippocampal and plasmatic lipids due to LPS treatment in mice. Thus, systemic inflammation induced by LPS in mice resulted in statistically significant increase in several cortical PCs/PEs (PC aa C33:3/PE aa C36:3, PC ae C34:3/PE ae C37:3, PC aa C34:2/PE aa C37:29, PC ae C34:2/PE ae C37:2) hippocampal PCs/PEs (PC ae C34:2/PE ae C37:2) and plasmatic lipids (PC(P-36:2)/PC(O-36:3), PC(P-34:1)/PC(O-34:1)/PE(P-37:1)/PE(O-37:2), PC(P-34:0)/PC(O-34:1)/PE(P-37:0)/PE(O-37:1) and glucosylceramide GlcCer(34:1)). However, as we did not distinguish these PCs/PEs, the future studies should investigate the changes in specific lipids and pathways regulating the observed changes.

Changes in protein expression in the brain

While the brain levels of neurotransmitters (i.e. glutamate, glutamine) were not disturbed due to LPS-induced inflammation, the absolute protein expression of glutamate *N*-methyl-D-aspartate (NMDA) receptor subunit GluN1 in the mouse brain cortex significantly increased after LPS treatment. The GluN1, which is highly expressed in the brain, acts as an obligatory subunit of functional NMDA receptors, which are ionotropic glutamate receptors with an crucial role in mediating excitatory neurotransmission (Hansen et al., 2018). The activation of synaptic NMDARs initiates plasticity and stimulates cell survival, while the activation of extrasynaptic NMDARs leads to cell death. Interestingly, Rosi et al (2004) demonstrated that chronic LPS-induced inflammation in the rat brain resulted in a decrease in the number of GluN1 receptors in the dentate gyrus and cornu ammonis 3 hippocampal areas, without any loss of neurons (Rosi et al., 2004). Moreover, GluN1 expression was significantly decreased in the brain cortex of APdE9 mice chronically treated with LPS compared to the wild type control mice, while no changes were observed in LPS treated wild-type mice (Puris et al., 2021a). All together, these results suggest that changes in GluN1 receptor expression in the brain are model-specific and dependent on LPS treatment regimen.

We investigated the changes in the brain cortical protein expression of ABC and SLC transporters, which are responsible for the passage of nutrients, metabolites and xenobiotics including drugs across the blood-brain barrier and within the brain. Previous studies demonstrated different changes in expression and function of these transporters into inflammation-associated diseases such as AD, Parkinson's disease and epilepsy indicating their potential involvement in the disease progression (Kooij et al., 2012, Pereira et al., 2018, Jia et al., 2020). The present study did not reveal statistically significant changes in protein expression of the efflux transporters P-gp, Mrp1, Mrp4, Bcrp, and nutrient transporters Glut1 and Lat1 due to systemic inflammation induced by LPS in mice. The results are similar to our previous report on non-altered protein expression of the mentioned transporters after chronic LPS treatment in 16-17-months-old mice (Puris et al., 2021a). Importantly, the levels of amino acids, substrates of Lat1 (i.e. phenylalanine, tryptophan, methionine, lysine, tyrosine), were not altered in the brain and plasma of the LPS-induced inflammation mouse model compared to saline-treated controls providing an evidence that both expression and function of Lat1 is not altered due to systemic inflammation induced by LPS in mice.

The expression of two other proteins associated with inflammation-related neurological diseases such as Mgl1 and Cox-2 (Berry et al., 2020, Guan and Wang, 2019) was not affected in the brain cortex by LPS-induced systemic inflammation. Mgl1 is a serine hydrolase which converts endocannabinoid 2-arachidonoyl-*sn*-glycerol to arachidonic acid, which is a precursor for the synthesis of neuroinflammatory prostaglandins mediated by Cox enzymes (Guan and Wang, 2019, Berry et al., 2020). In the brain, Cox-2 mediates the production of prostaglandins, such as prostaglandin E₂ (PGE₂), which binds to its receptors and results in the release of inflammatory mediators, including IL-1 β , IL-6 and TNF α (Sil and Ghosh, 2016). The production of these cytokines was not detected in the brain cortical tissue in the investigated models. In addition, the levels of arachidonic acid in the brain cortex and hippocampus were similar in the LPS-treated mice compared to those in saline-treated animals. These findings support the evidence that Mgl1- and Cox-2-mediated pathways are not activated in the brain cortex in the LPS-induced inflammation mice used in the present study. Similarly, the expression of Mgl1 and Cox-2 in the brain cortical tissue did not differ between the 16-17-months-old mice chronically treated with LPS and age-matched controls (Puris et al., 2021a). However, as we observed microglial and astrocytic activation as well as increased expression of β - and γ -secretases in the hippocampus, but not in the cortex of the LPS-treated mice, future studies should focus on investigation of changes in protein expression of Mgl1, Cox-2 and other proteins in the hippocampus.

Limitations and future perspectives

In the present study, we investigate general changes in the metabolome and lipidome as well as the protein expression of several proteins in LPS-induced inflammation mouse model in order to give insight about the altered biochemical pathways. Therefore, the future studies should be performed to elucidate the specific pathways altered in inflammation. The changes in the brain cortical and hippocampal tissue revealed in the present study represent the pool of all brain parenchymal cells and the changes cannot be attributed to specific parenchymal cells. Moreover, the study results highlighted the importance of investigation of the brain region-specific alterations in inflammatory conditions. Thus, the cell-specific alterations due to inflammation should be investigated in the future studies. In addition, many metabolites in this study were below the detection /quantification limits of current analytical protocols and/or are not present in the spectral libraries. It makes their analysis challenging and future experiments should focus on the study of specific metabolites and pathways.

In conclusion, in the present comprehensive -omics study, we reported the short-term effects of systemic inflammation induced by LPS administration on the mouse plasma and brain cortical and hippocampal metabolome, lipidome as well as expression of the brain cortical proteins which were shown to be involved in inflammation-associated CNS diseases. The study revealed several brain region-specific changes in metabolic pathways and lipids. Importantly, LPS administration in mice resulted in significantly increased protein expression of GluN1 receptor in the brain cortex. The revealed disturbances in the LPS-induced inflammation mouse model may provide insight into the mechanisms underlying inflammation-associated CNS diseases as well as the appropriate use of this model during target validation and drug candidate testing.

Data availability

All the data generated or analysed during the study are included in this published article and its supplementary information files.

Acknowledgements

This work was supported by the Finnish Cultural Foundation, the Emil Aaltonen Foundation, the Alexander von Humboldt Foundation, the Czech Science Foundation Grant [18-12204S], and MH CZ—DRO (FNOL, 00098892). The authors thank Mr. Casas Mon, Ms. Giménez, Prof. Korhonen, Ms. Schroth, Ms. Leal Estrada and Ms. Reponen for technical assistance in sample preparation and Dr. Petsalo and Dr. Huttunen for help in building the collaboration between institutions. The University of Eastern Finland analytical laboratory is supported by Biocenter Finland and Biocenter Kuopio.

References

- ALEXANDER, C. & RIETSCHL, E. T. 2001. Bacterial lipopolysaccharides and innate immunity. *J Endotoxin Res*, 7, 167-202.
- BERRY, A. J., ZUBKO, O., REEVES, S. J. & HOWARD, R. J. 2020. Endocannabinoid system alterations in Alzheimer's disease: A systematic review of human studies. *Brain Res*, 1749, 147135.
- BEUTLER, B. 2000. Tlr4: central component of the sole mammalian LPS sensor. *Curr Opin Immunol*, 12, 20-6.
- CANI, P. D., AMAR, J., IGLESIAS, M. A., POGGI, M., KNAUF, C., BASTELICA, D., NEYRINCK, A. M., FAVA, F., TUOHY, K. M., CHABO, C., WAGET, A., DELMEE, E., COUSIN, B., SULPICE, T., CHAMONTIN, B., FERRIERES, J., TANTI, J. F., GIBSON, G. R., CASTEILLA, L., DELZENNE, N. M., ALESSI, M. C. & BURCELIN, R. 2007. Metabolic endotoxemia initiates obesity and insulin resistance. *Diabetes*, 56, 1761-72.
- CATORCE, M. N. & GEVORKIAN, G. 2016. LPS-induced Murine Neuroinflammation Model: Main Features and Suitability for Pre-clinical Assessment of Nutraceuticals. *Curr Neuropharmacol*, 14, 155-64.
- COULSON, D. T., BEYER, N., QUINN, J. G., BROCKBANK, S., HELLEMANS, J., IRVINE, G. B., RAVID, R. & JOHNSTON, J. A. 2010. BACE1 mRNA expression in Alzheimer's disease postmortem brain tissue. *J Alzheimers Dis*, 22, 1111-22.
- DISABATO, D. J., QUAN, N. & GODBOUT, J. P. 2016. Neuroinflammation: the devil is in the details. *J Neurochem*, 139 Suppl 2, 136-153.
- DUNN, W. B., BROADHURST, D., BEGLEY, P., ZELENA, E., FRANCIS-MCINTYRE, S., ANDERSON, N., BROWN, M., KNOWLES, J. D., HALSALL, A., HASELDEN, J. N., NICHOLLS, A. W., WILSON, I. D., KELL, D. B., GOODACRE, R. & HUMAN SERUM METABOLOME, C. 2011. Procedures for large-scale metabolic profiling of serum and plasma using gas chromatography and liquid chromatography coupled to mass spectrometry. *Nat Protoc*, 6, 1060-83.
- GHOSH, A., COMEROTA, M. M., WAN, D., CHEN, F., PROPSON, N. E., HWANG, S. H., HAMMOCK, B. D. & ZHENG, H. 2020. An epoxide hydrolase inhibitor reduces neuroinflammation in a mouse model of Alzheimer's disease. *Sci Transl Med*, 12.
- GILHUS, N. E. & DEUSCHL, G. 2019. Neuroinflammation - a common thread in neurological disorders. *Nat Rev Neurol*, 15, 429-430.
- GIRIDHARAN, V. V., MASUD, F., PETRONILHO, F., DAL-PIZZOL, F. & BARICHELLO, T. 2019. Infection-Induced Systemic Inflammation Is a Potential Driver of Alzheimer's Disease Progression. *Front Aging Neurosci*, 11, 122.
- GUAN, P. P. & WANG, P. 2019. Integrated communications between cyclooxygenase-2 and Alzheimer's disease. *FASEB J*, 33, 13-33.
- HANSEN, K. B., YI, F., PERSZYK, R. E., FURUKAWA, H., WOLLMUTH, L. P., GIBB, A. J. & TRAYNELIS, S. F. 2018. Structure, function, and allosteric modulation of NMDA receptors. *J Gen Physiol*, 150, 1081-1105.
- HOLMES, C., EL-OKL, M., WILLIAMS, A. L., CUNNINGHAM, C., WILCOCKSON, D. & PERRY, V. H. 2003. Systemic infection, interleukin 1beta, and cognitive decline in Alzheimer's disease. *J Neurol Neurosurg Psychiatry*, 74, 788-9.
- IYER, S. S., ACCARDI, C. J., ZIEGLER, T. R., BLANCO, R. A., RITZENTHALER, J. D., ROJAS, M., ROMAN, J. & JONES, D. P. 2009. Cysteine redox potential determines pro-inflammatory IL-1beta levels. *PLoS One*, 4, e5017.
- JIA, Y., WANG, N., ZHANG, Y., XUE, D., LOU, H. & LIU, X. 2020. Alteration in the Function and Expression of SLC and ABC Transporters in the Neurovascular Unit in Alzheimer's Disease and the Clinical Significance. *Aging Dis*, 11, 390-404.
- JONES, L. L., MCDONALD, D. A. & BORUM, P. R. 2010. Acylcarnitines: role in brain. *Prog Lipid Res*, 49, 61-75.

- KOOIJ, G., VAN HORSSSEN, J., BANDARU, V. V., HAUGHEY, N. J. & DE VRIES, H. E. 2012. The Role of ATP-Binding Cassette Transporters in Neuro-Inflammation: Relevance for Bioactive Lipids. *Front Pharmacol*, 3, 74.
- KOURIL, S., DE SOUSA, J., VACLAVIK, J., FRIEDECKY, D. & ADAM, T. 2020. CROP: correlation-based reduction of feature multiplicities in untargeted metabolomic data. *Bioinformatics*, 36, 2941-2942.
- KWON, H. S. & KOH, S. H. 2020. Neuroinflammation in neurodegenerative disorders: the roles of microglia and astrocytes. *Transl Neurodegener*, 9, 42.
- LEE, J. W., LEE, Y. K., YUK, D. Y., CHOI, D. Y., BAN, S. B., OH, K. W. & HONG, J. T. 2008. Neuro-inflammation induced by lipopolysaccharide causes cognitive impairment through enhancement of beta-amyloid generation. *J Neuroinflammation*, 5, 37.
- LEHNARDT, S., LACHANCE, C., PATRIZI, S., LEFEBVRE, S., FOLLETT, P. L., JENSEN, F. E., ROSENBERG, P. A., VOLPE, J. J. & VARTANIAN, T. 2002. The toll-like receptor TLR4 is necessary for lipopolysaccharide-induced oligodendrocyte injury in the CNS. *J Neurosci*, 22, 2478-86.
- LI, T., LI, Y. M., AHN, K., PRICE, D. L., SISODIA, S. S. & WONG, P. C. 2011. Increased expression of PS1 is sufficient to elevate the level and activity of gamma-secretase in vivo. *PLoS One*, 6, e28179.
- LI, T., ZHENG, L. N. & HAN, X. H. 2020. Fenretinide attenuates lipopolysaccharide (LPS)-induced blood-brain barrier (BBB) and depressive-like behavior in mice by targeting Nrf-2 signaling. *Biomed Pharmacother*, 125, 109680.
- LI, W., ALI, T., ZHENG, C., LIU, Z., HE, K., SHAH, F. A., REN, Q., RAHMAN, S. U., LI, N., YU, Z. J. & LI, S. 2021. Fluoxetine regulates eEF2 activity (phosphorylation) via HDAC1 inhibitory mechanism in an LPS-induced mouse model of depression. *J Neuroinflammation*, 18, 38.
- MAITRA, U., DENG, H., GLAROS, T., BAKER, B., CAPELLUTO, D. G., LI, Z. & LI, L. 2012. Molecular mechanisms responsible for the selective and low-grade induction of proinflammatory mediators in murine macrophages by lipopolysaccharide. *J Immunol*, 189, 1014-23.
- MANOUCHEHRIAN, O., RAMOS, M., BACHILLER, S., LUNDGAARD, I. & DEIERBORG, T. 2021. Acute systemic LPS-exposure impairs perivascular CSF distribution in mice. *J Neuroinflammation*, 18, 34.
- MRAK, R. E. & GRIFFIN, W. S. 2005. Glia and their cytokines in progression of neurodegeneration. *Neurobiol Aging*, 26, 349-54.
- MU, Y. & GAGE, F. H. 2011. Adult hippocampal neurogenesis and its role in Alzheimer's disease. *Mol Neurodegener*, 6, 85.
- OBEID, R. 2013. The metabolic burden of methyl donor deficiency with focus on the betaine homocysteine methyltransferase pathway. *Nutrients*, 5, 3481-95.
- PAN, Y., OMORI, K., ALI, I., TACHIKAWA, M., TERASAKI, T., BROUWER, K. L. R. & NICOLAZZO, J. A. 2018. Altered Expression of Small Intestinal Drug Transporters and Hepatic Metabolic Enzymes in a Mouse Model of Familial Alzheimer's Disease. *Mol Pharm*, 15, 4073-4083.
- PAN, Y., OMORI, K., ALI, I., TACHIKAWA, M., TERASAKI, T., BROUWER, K. L. R. & NICOLAZZO, J. A. 2019. Increased Expression of Renal Drug Transporters in a Mouse Model of Familial Alzheimer's Disease. *J Pharm Sci*, 108, 2484-2489.
- PAWLOWSKY-GLAHN, V. & BUCCIANTI, A. 2011. *Compositional data analysis: Theory and applications*, Chichester, Wiley.
- PEREIRA, C. D., MARTINS, F., WILTFANG, J., DA CRUZ, E. S. O. A. B. & REBELO, S. 2018. ABC Transporters Are Key Players in Alzheimer's Disease. *J Alzheimers Dis*, 61, 463-485.
- PIIRSALU, M., TAALBERG, E., LILLEVALI, K., TIAN, L., ZILMER, M. & VASAR, E. 2020. Treatment With Lipopolysaccharide Induces Distinct Changes in Metabolite Profile and Body Weight in 129Sv and B16 Mouse Strains. *Front Pharmacol*, 11, 371.
- PURIS, E., AURIOLA, S., KORHONEN, P., LOPPI, S., KANNINEN, K. M., MALM, T., KOISTINAHO, J. & GYNTHNER, M. 2021a. Systemic Inflammation Induced Changes

- in Protein Expression of ABC Transporters and Ionotropic Glutamate Receptor Subunit 1 in the Cerebral Cortex of Familial Alzheimer's Disease Mouse Model. *J Pharm Sci*.
- PURIS, E., KOURIL, S., NAJDEKR, L., LOPPI, S., KORHONEN, P., KANNINEN, K. M., MALM, T., KOISTINAHO, J., FRIEDECKY, D. & GYNTHNER, M. 2021b. Metabolomic and lipidomic changes triggered by lipopolysaccharide-induced systemic inflammation in transgenic APdE9 mice. *Sci Rep*, 11, 13076.
- ROSI, S., RAMIREZ-AMAYA, V., HAUSS-WEGRZYNIAK, B. & WENK, G. L. 2004. Chronic brain inflammation leads to a decline in hippocampal NMDA-R1 receptors. *J Neuroinflammation*, 1, 12.
- SARAFIAN, M. H., GAUDIN, M., LEWIS, M. R., MARTIN, F. P., HOLMES, E., NICHOLSON, J. K. & DUMAS, M. E. 2014. Objective set of criteria for optimization of sample preparation procedures for ultra-high throughput untargeted blood plasma lipid profiling by ultra performance liquid chromatography-mass spectrometry. *Anal Chem*, 86, 5766-74.
- SELHUB, J., BAGLEY, L. C., MILLER, J. & ROSENBERG, I. H. 2000. B vitamins, homocysteine, and neurocognitive function in the elderly. *Am J Clin Nutr*, 71, 614S-620S.
- SIL, S. & GHOSH, T. 2016. Role of cox-2 mediated neuroinflammation on the neurodegeneration and cognitive impairments in colchicine induced rat model of Alzheimer's Disease. *J Neuroimmunol*, 291, 115-24.
- SLY, L. M., KRZESICKI, R. F., BRASHLER, J. R., BUHL, A. E., MCKINLEY, D. D., CARTER, D. B. & CHIN, J. E. 2001. Endogenous brain cytokine mRNA and inflammatory responses to lipopolysaccharide are elevated in the Tg2576 transgenic mouse model of Alzheimer's disease. *Brain Res Bull*, 56, 581-8.
- TEAM, R. C. 2013. R: A Language and Environment for Statistical Computing.
- UCHIDA, Y., OHTSUKI, S., KATSUKURA, Y., IKEDA, C., SUZUKI, T., KAMIIE, J. & TERASAKI, T. 2011. Quantitative targeted absolute proteomics of human blood-brain barrier transporters and receptors. *J Neurochem*, 117, 333-45.
- UCHIDA, Y., TACHIKAWA, M., OBUCHI, W., HOSHI, Y., TOMIOKA, Y., OHTSUKI, S. & TERASAKI, T. 2013. A study protocol for quantitative targeted absolute proteomics (QTAP) by LC-MS/MS: application for inter-strain differences in protein expression levels of transporters, receptors, claudin-5, and marker proteins at the blood-brain barrier in ddY, FVB, and C57BL/6J mice. *Fluids Barriers CNS*, 10, 21.
- VORKAS, P. A., ISAAC, G., ANWAR, M. A., DAVIES, A. H., WANT, E. J., NICHOLSON, J. K. & HOLMES, E. 2015. Untargeted UPLC-MS profiling pipeline to expand tissue metabolome coverage: application to cardiovascular disease. *Anal Chem*, 87, 4184-93.
- WU, Y., FU, Y., RAO, C., LI, W., LIANG, Z., ZHOU, C., SHEN, P., CHENG, P., ZENG, L., ZHU, D., ZHAO, L. & XIE, P. 2016. Metabolomic analysis reveals metabolic disturbances in the prefrontal cortex of the lipopolysaccharide-induced mouse model of depression. *Behav Brain Res*, 308, 115-27.
- YUAN, M., BREITKOPF, S. B., YANG, X. & ASARA, J. M. 2012. A positive/negative ion-switching, targeted mass spectrometry-based metabolomics platform for bodily fluids, cells, and fresh and fixed tissue. *Nat Protoc*, 7, 872-81.
- ZHAO, C., DENG, W. & GAGE, F. H. 2008. Mechanisms and functional implications of adult neurogenesis. *Cell*, 132, 645-60.
- ZHAO, G., HE, F., WU, C., LI, P., LI, N., DENG, J., ZHU, G., REN, W. & PENG, Y. 2018. Betaine in Inflammation: Mechanistic Aspects and Applications. *Front Immunol*, 9, 1070.
- ZHAO, J., BI, W., XIAO, S., LAN, X., CHENG, X., ZHANG, J., LU, D., WEI, W., WANG, Y., LI, H., FU, Y. & ZHU, L. 2019. Neuroinflammation induced by lipopolysaccharide causes cognitive impairment in mice. *Sci Rep*, 9, 5790.

ZONIS, S., PECHNICK, R. N., LJUBIMOV, V. A., MAHGEREFTEH, M., WAWROWSKY, K., MICHELSEN, K. S. & CHESNOKOVA, V. 2015. Chronic intestinal inflammation alters hippocampal neurogenesis. *J Neuroinflammation*, 12, 65.

Journal Pre-proofs

Figure legends

Figure 1. (A) Box-and-whisker plots of levels of interleukins (IL-6, IL-10, IL-12p70), interferon- γ (IFN- γ), monocyte chemoattractant protein-1 (MCP-1) and tumour necrosis factor α (TNF- α) in spleen of the saline-treated wild-type (WT) control mice ($n = 6$) versus WT mice treated with LPS ($n = 7$). (B) The comparison of levels of IL-6, IL-10, MCP-1, IFN- γ , TNF- α and IL-12p70 in plasma of wild-type WT control mice ($n = 8$) and WT mice treated with LPS ($n = 8$). The boxes represent the interquartile range (IQR) defined by the 25th and 75th percentiles. The horizontal line represents the median value. The upper whisker and lower whisker represents 5th and 95th percentile. Asterisks denote a statistically significant difference from the respective control ($*p < 0.05$, $** < 0.01$, unpaired t -test).

Figure 2. Normalized fold mRNA expression of glial fibrillary acidic protein (Gfap), allograft inflammatory factor 1 (Aif1), β -secretase 1 (Bace1), Presenilin-1 (Psen1), γ -secretase subunit APH-1A (Aph1a) and γ -secretase subunit APH-1B (Aph1b) in the brain hippocampal (A) and cortical (B) tissues of the saline-treated wild-type (WT) control mice ($n = 4$) and WT mice treated with LPS (WT plus LPS) ($n = 4$). The gene expression was normalized against the β -actin house-keeping gene. The data is presented as mean \pm SD. Asterisks denote a statistically significant difference from the respective control ($*p < 0.05$, $** < 0.01$, unpaired t -test).

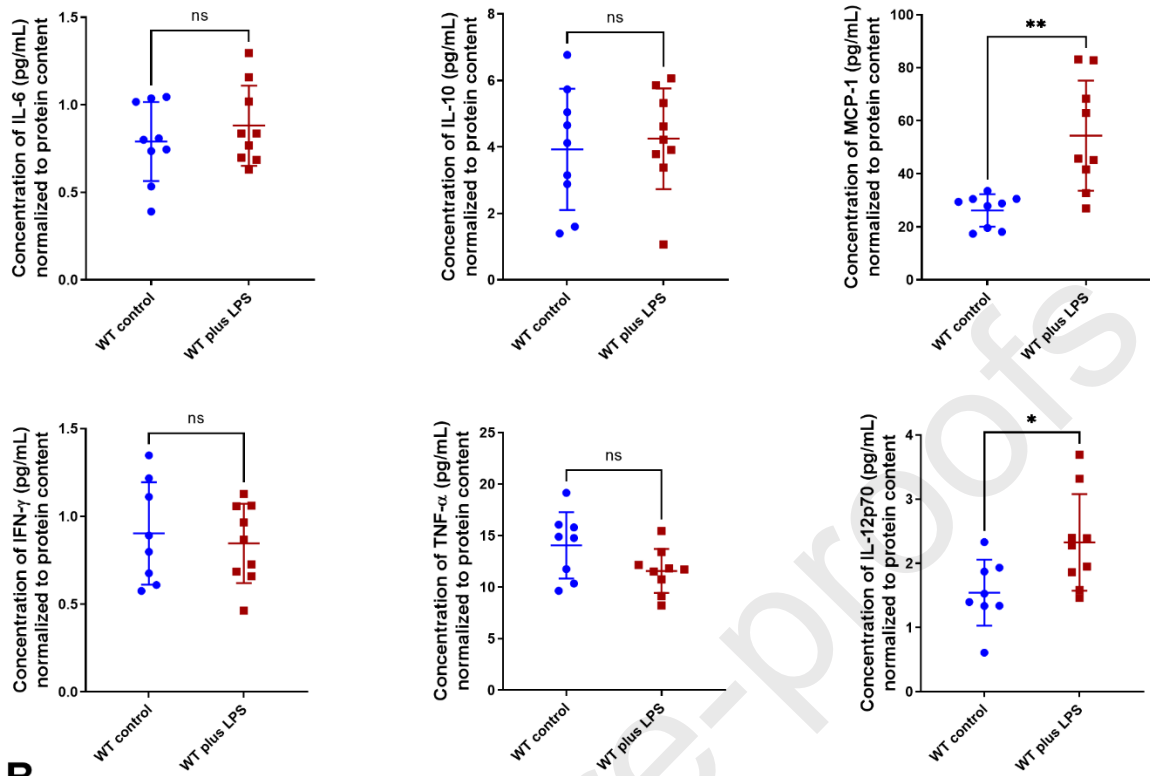
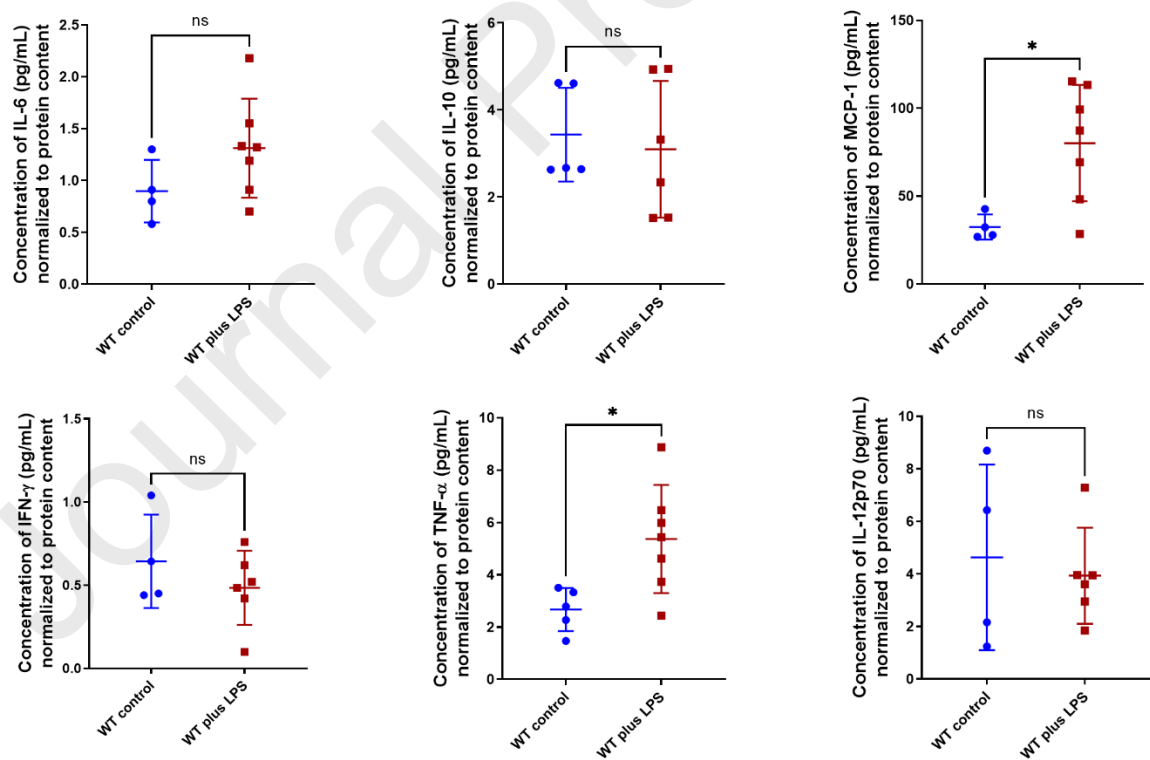
Figure 3. Principal component analysis (PCA) score plots for each model and analytical approach studied to compare global differences in the metabolomic (A-C) and lipid composition (D-F) of the brain hippocampus, cortex and plasma in the saline-treated wild-type (WT) control mice ($n = 9$) and WT mice treated with LPS (WT plus LPS) ($n = 9$).

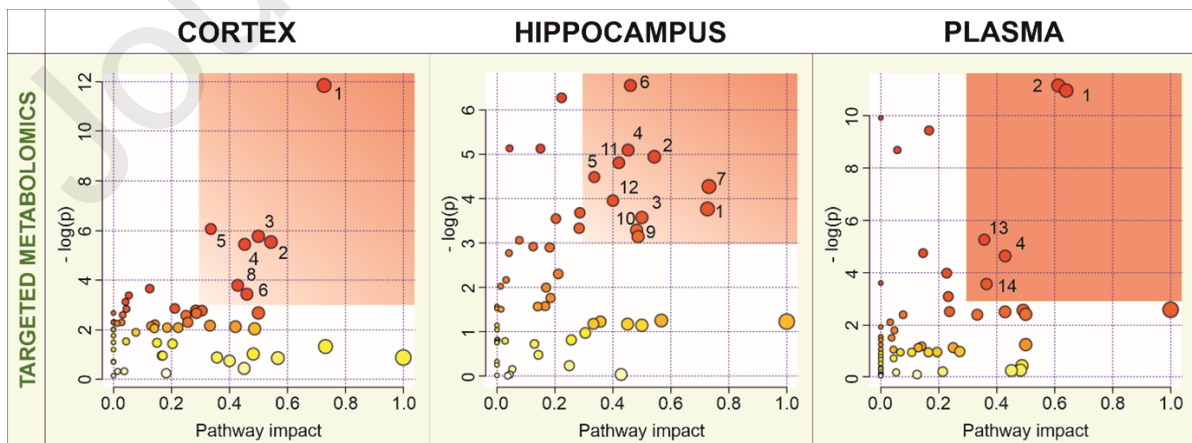
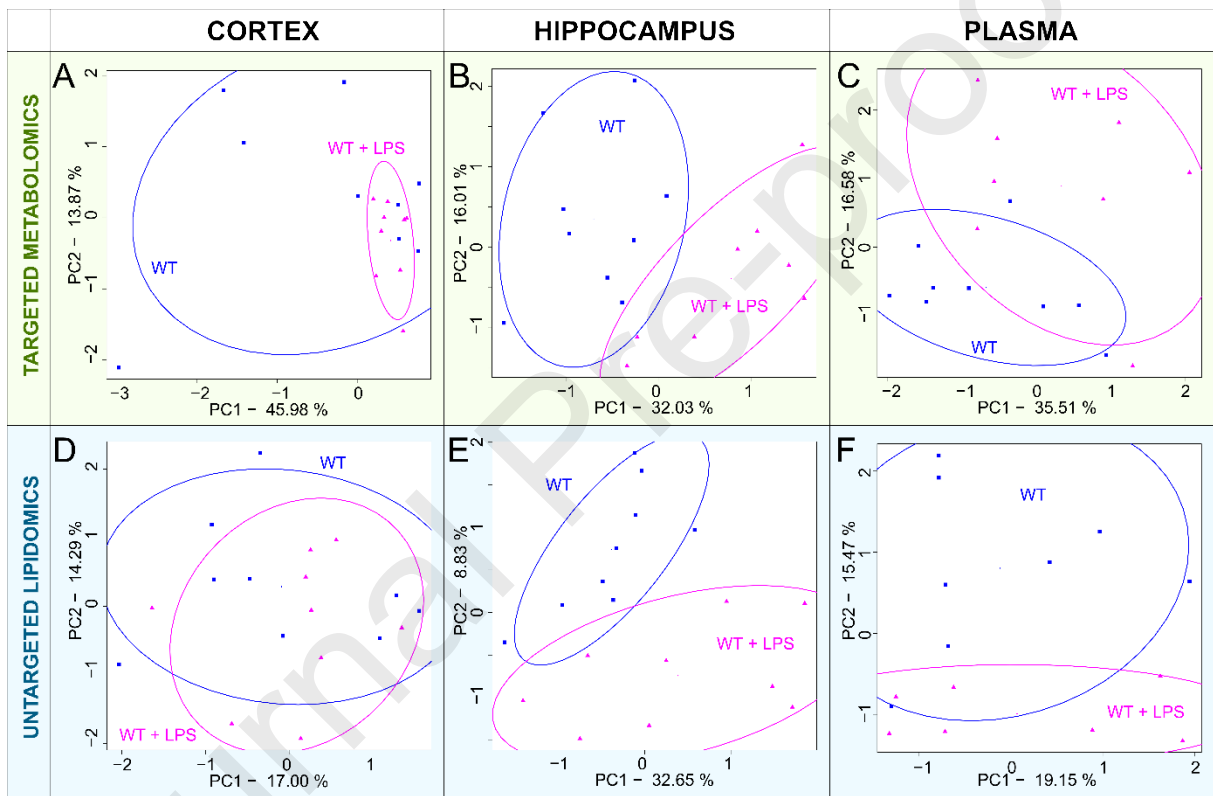
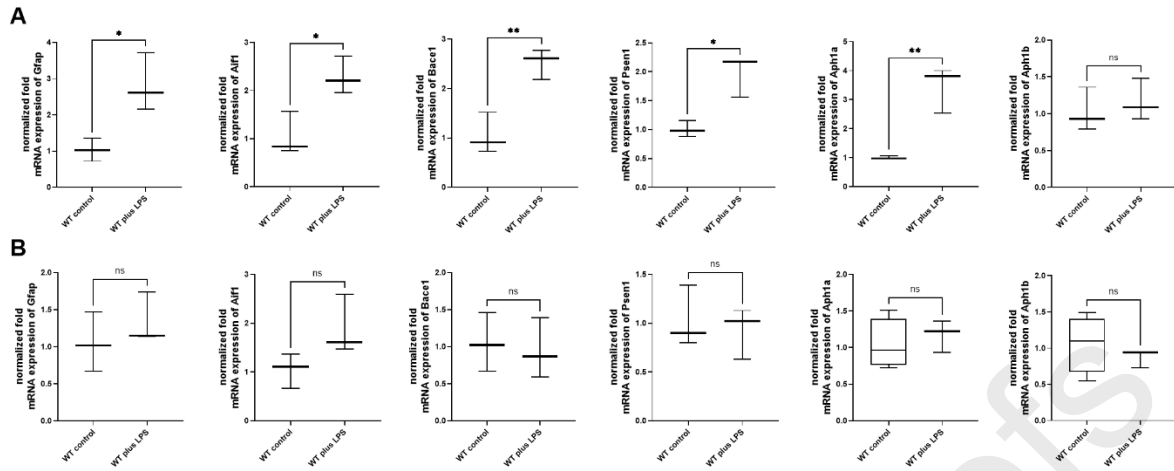
Figure 4. Biochemical pathway analysis performed on targeted metabolomic data in the brain hippocampus, cortex and plasma of the wild-type (WT) mice treated with LPS ($n = 9$) versus the respective saline-treated WT controls ($n = 9$). The red rectangle highlights the most affected pathways with $-\log(p\text{-value})$ greater than 3 and a pathway impact greater than 0.3 for all graphs. Individual pathways are numbered as follows: 1 – glycine, serine, and threonine metabolism, 2 – cysteine and methionine metabolism, 3 – riboflavin metabolism, 4 – arginine and proline metabolism, 5 – pyrimidine metabolism, 6 – nicotinate and nicotinamide metabolism, 7 – alanine, aspartate, and glutamate metabolism, 8 – taurine and hypotaurine metabolism, 9 – carbohydrate metabolism, 10 – arginine biosynthesis, 11 – purine metabolism, 12 – glutathione metabolism, 13 – phenylalanine metabolism, 14 – citrate cycle (TCA cycle).

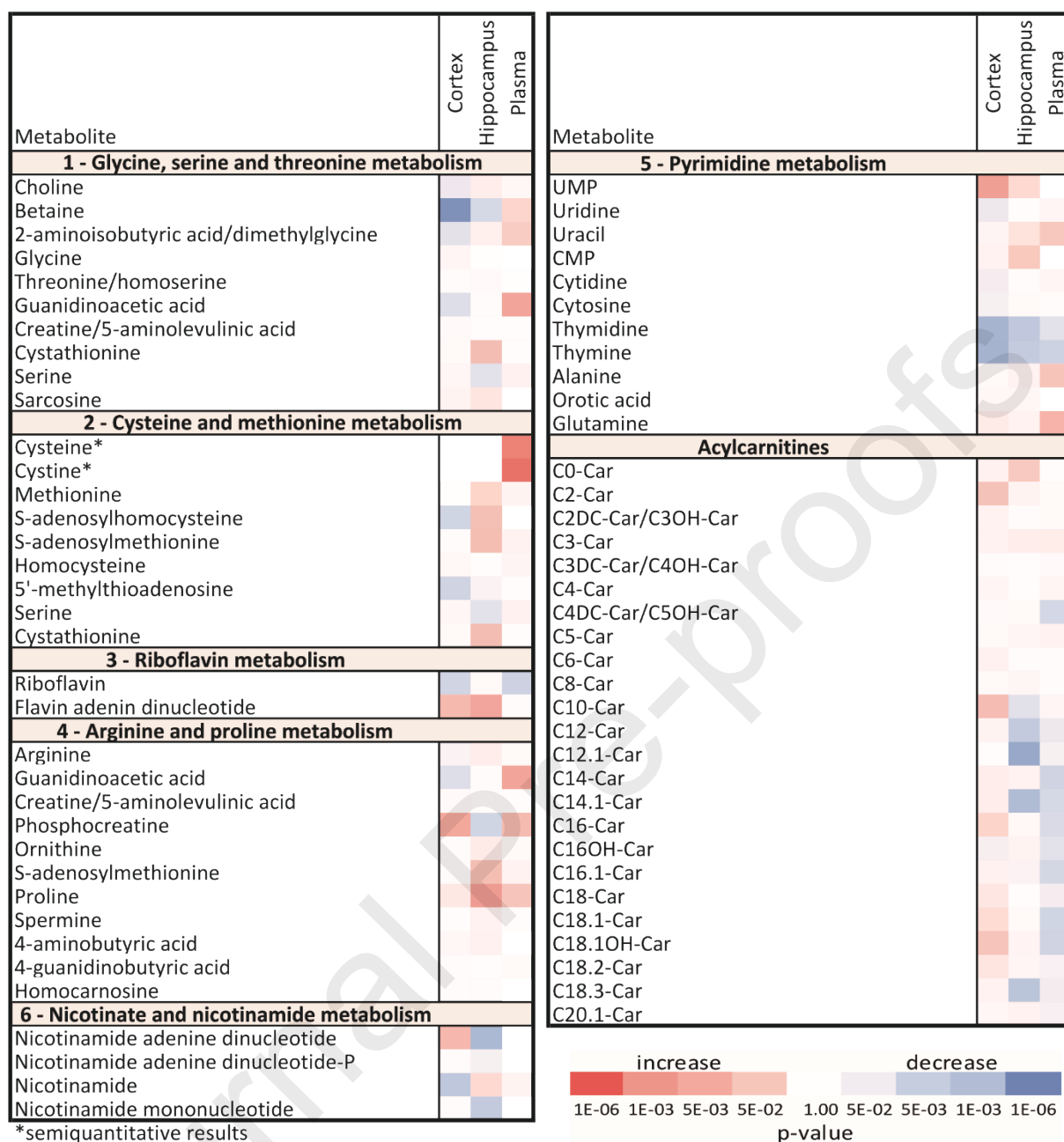
Figure 5. The heatmap of statistically significant and successfully annotated compounds represents the changes in metabolite levels in the brain cortex, hippocampus and plasma of the wild-type control mice (WT) treated with LPS ($n = 9$) versus saline-treated WT controls ($n =$

9). Heatmap of p -values without correction, $-\log_{10}$ scaled: red – increased metabolites (fold-change > 0), blue – decreased metabolites (fold-change < 0). The statistical significance on the level of 0.05 after Bonferroni correction was calculated as a p -value $< 3.23 \times 10^{-4}$. Details of the metabolites are provided in Supplementary Tables S4 and S6.

Figure 6. The heatmap of statistically significant and successfully annotated compounds represents the changes in the most affected lipid levels in the cortex and hippocampus of the wild-type control mice (WT) treated with LPS ($n = 9$) versus saline-treated WT controls ($n = 9$). Heatmap of p -values without correction $-\log_{10}$ scaled, red – increased lipids (fold-change > 0), blue – decreased lipids (fold-change < 0). The statistical significance after Bonferroni correction was considered as a p -value $< 3.48 \times 10^{-5}$. Details of the metabolites are provided in Supplementary Table S5.

A**B**





- LPS-induced inflammation led to decreased levels of brain cortical betaine in mice
- Increased levels of several cortical PCs/PEs were found in mice treated with LPS
- LPS treatment induced GluN1 receptor protein expression in the mouse brain cortex

Journal Pre-proofs